FEMS Yeast Research, 18, 2018, foy011

doi: 10.1093/femsyr/foy011
Advance Access Publication Date: 21 June 2018
Research Article

RESEARCH ARTICLE

Spathaspora passalidarum selected for resistance to AFEX hydrolysate shows decreased cell yield

Yi-Kai Su[1,2,3,4,*], Laura B. Willis[2,3,5], Lars Rehmann[4], David R. Smith[6,†] and Thomas W. Jeffries[2,3,5]

[1]Department of Biological Systems Engineering, University of Wisconsin, Madison, WI 53706, USA, [2]DOE Great Lakes Bioenergy Research Center, University of Wisconsin, Madison, WI 53705, USA, [3]Forest Products Laboratory, USDA Forest Service, Madison, WI, 53726, USA, [4]Department of Chemical and Biochemical Engineering, University of Western Ontario, London, ON, N6A 3K, Canada, [5]Department of Bacteriology, University of Madison, WI, 53705, USA and [6]Department of Biology, University of Western Ontario, London, ON, N6A 3K7, Canada

*Corresponding author: Department of Biological Systems Engineering, University of Wisconsin - Madison 460 Henry Mall, Madison, WI 53706, USA. Tel: +1(519)-694-5159; yikai.su@wisc.edu

One sentence summary: This paper describes how a mutant strain of *Spathaspora passalidarum* shows reduced respiration and increased resistance to toxins from cellulosic hydrolysate.

Editor: Jens Nielsen

†David R. Smith, http://orcid.org/0000-0001-9560-5210

ABSTRACT

This study employed cell recycling, batch adaptation, cell mating and high-throughput screening to select adapted *Spathaspora passalidarum* strains with improved fermentative ability. The most promising candidate YK208-E11 (E11) showed a 3-fold increase in specific fermentation rate compared to the parental strain and an ethanol yield greater than 0.45 g/g substrate while co-utilizing cellobiose, glucose and xylose. Further characterization showed that strain E11 also makes 40% less biomass compared to the parental strain when cultivated in rich media under aerobic conditions. A tetrazolium agar overlay assay in the presence of respiration inhibitors, including rotenone, antimycin A, KCN and salicylhydroxamic acid elucidated the nature of the mutational events. Results indicated that E11 has a deficiency in its respiration system that could contribute to its low cell yield. Strain E11 was subjected to whole genome sequencing and an ~11 kb deletion was identified; the open reading frames absent in strain E11 code for proteins with predicted functions in respiration, cell division and the actin cytoskeleton, and may contribute to the observed physiology of the adapted strain. Results of the tetrazolium overlay also suggest that cultivation on xylose affects the respiration capacity in the wild-type strain, which could account for its faster fermentation of xylose as compared to glucose. These results support our previous finding that *S. passalidarum* has highly unusual physiological responses to xylose under oxygen limitation.

Keywords: *Spathaspora passalidarum*; lignocellulosic fermentation; adaptation; evolutionary engineering; tetrazolium assay; respiration inhibitor

ABBREVIATIONS

AA:	antimycin A
AA + SH:	antimycin A plus salicylhydroxamic acid
AFEX:	ammonia fiber expansion
AFCS:	AFEX-pretreated corn stover hydrolysate
AFCS-RO:	AFEX hydrolysate treated with reverse osmosis
AOX:	alternative oxidase
CDW:	cell dry weight

Received: 22 July 2016; **Accepted:** 20 June 2018

HMF: 5-hydroxyl methylfurfural
OD_{600}: optical density at 600 nm
TTC: tetrazolium chloride
ROT: rotenone
SHAM: salicylhydroxamic acid
STO: SHAM-sensitive terminal oxidase

INTRODUCTION

Spathaspora passalidarum NN245 is an unusual yeast that shows a high capacity for fermenting xylose, cellobiose and glucose from pure sugars or from lignocellulosic hydrolysates (Long *et al.* 2012). The *Spathaspora* genus (Cadete *et al.* 2009, 2013; Lopes *et al.* 2016) is closely related to the *Scheffersomyces* clade (Urbina and Blackwell 2012) and shares with it a proclivity for living in the hindgut of larva and adult wood-boring beetles of the family Passalidae (Nardi *et al.* 2006; Urbina, Schuster and Blackwell 2013). The physiology of *S. passalidarum* is still poorly understood, even though its genome has been sequenced (Wohlbach *et al.* 2011). One of its more unusual features is that it appears to be capable of growth with very little oxygen (Hou 2012), and it shows about 40% less cell growth and higher specific rates of ethanol production when grown on xylose vs glucose (Long *et al.* 2012; Su, Willis and Jeffries 2015). These characteristics make it potentially useful for bioconversion.

However, like other microorganisms, *S. passalidarum* growth and fermentation are inhibited by toxic chemicals such as weak organic acids (e.g. acetic acid, levulinic acid and formic acid), 5-hydroxyl methylfurfural (HMF), furfural and phenolic compounds found in lignocellulosic hydrolysates (Palmqvist and Hahn-Hagerdal 2000; Almeida *et al.* 2011; Ask *et al.* 2013). Acetic acid is released by hydrolyzing the acetyl side chain on the xylan backbone, while levulinic acid and formic acid are formed by further dehydrating HMF and furfural (Klinke, Thomsen and Ahring 2004). Two inhibitory mechanisms of weak acids were proposed: (i) intracellular anion accumulation and (ii) uncoupling of ATPase due to the increasing H^+ concentration in the cytosol (Palmqvist and Hahn-Hagerdal 2000). Weak acids reduce cell growth, hinder xylose uptake and inhibit carbohydrate metabolism (Casey *et al.* 2010; Mira, Teixeira and Sa-Correia 2010; Hasunuma *et al.* 2011). Furfural and HMF cause slower growth and longer lag phase in yeasts (Palmqvist and Hahn-Hagerdal 2000). Allen *et al.* (2010) demonstrated that furfural induces the accumulation of reactive oxygen species, which can damage the chromatin and prevent cell proliferation.

Phenolic compounds and their derivatives (e.g. 4-hydroxybenzaldehyde, vanillin, *p*-coumaric acid and ferulic acid) arise from partial degradation of lignocellulose (Klinke, Thomsen and Ahring 2004). Phenolic compounds are lipophilic; thus, they can diffuse into the cell membrane and affect its selectivity and integrity as enzyme matrices (Palmqvist and Hahn-Hagerdal 2000). Larsson *et al.* (2000) showed that even 5 mM of *p*-coumaric acid or ferulic acid can severely inhibit *S. cerevisiae* during glucose fermentation. Furthermore, the synergic effect of combining more than two toxic compounds is greater than the presence of individual one (Palmqvist and Hahn-Hagerdal 2000; Klinke, Thomsen and Ahring 2004). Several mechanisms have been proposed for inhibition and detoxification; for example, presence of a multidrug resistant transporter, ATP and reducing equivalent (e.g. NAD[P]H) are required for the detoxification process (Almeida *et al.* 2011; Jonsson, Alriksson and Nilvebrant 2013; Adeboye, Bettiga and Olsson 2014)

The toxicity of hydrolysate is a major barrier to commercializing lignocellulosic ethanol production. Directed evolution and empirical strain development have proven useful in reducing these problems. Successful approaches have included selecting for resistance to individual hydrolysate components such as acetic acid or furfural (Nilsson *et al.* 2005) or serial selection against successively higher concentrations of hydrolysate (Stoutenburg, Perrotta and Nakas 2011). Even though it is generally easier to select for resistance to individual components, the difficulty in knowing which are the most important or the possibility of synergistic toxicities arising from multiple inhibitors can favor the experimental approach of direct selection for resistance to successively higher concentrations of diluted hydrolysate (Hughes *et al.* 2012; Harner *et al.* 2014).

The overall aim of our study was to identify yeasts that would resist a wide range of inhibitors from various feedstocks and pretreatment processes. We hypothesized that the major inhibitors, such as acetic acid, furfural and HMF, would be present in most hydrolysates, albeit at various concentrations, and that selecting for resistance to one hydrolysate would help confer resistance to a hydrolysate with a different origin. We further hypothesized that by combining traits from separately selected and adapted populations, we would be able to identify isolated strains with favorable resistance traits over a wide range of hydrolysates. In this process, we focused on the use of enzymatic hydrolysates from ammonia fiber expansion (AFEX)-pretreated corn stover due to its availability.

After several rounds of selection and adaptation, we identified strains that were capable of growth in the presence of hydrolysate and retained the ability to co-utilize glucose, xylose and cellobiose in hydrolysate for ethanol production. One promising strain, YK208-E11 (E11), exhibited an ethanol productivity of 0.31 g/L · h, which was 1.7 times higher than the parent NN245 strain grown under the same conditions. To assess whether respiration functions remained intact in the adapted strain, we examined viability, growth rates and tetrazolium reactions when cells were grown on synthetic minimal medium containing respiration inhibitors, such as KCN, rotenone (ROT), antimycin A (AA) or salicylhydroxamic acid (SHAM), and then overlaying with tetrazolium chloride (TTC) agar. These tests suggested that the electron transport chain (ETC), specifically the ROT-resistant dehydrogenases, may be disrupted in strain E11. To further characterize strain E11, we subjected it to whole genome sequencing and identified a deletion of ~11 kb and a duplication region. Some open reading frames present in these genomic regions are predicted to encode proteins with functions in respiration, cell division and the actin cytoskeleton, and the observed genomic changes may contribute to the observed physiology of the adapted strain.

MATERIALS AND METHODS

Strains, evolutionary engineering and batch adaptation

The wild-type strain *S. passalidarum* NN245 (NRRL Y-27907) was used as the parental strain for the adaptation process. During adaptation, stocks of both the parental and evolved strains were maintained in 15% sterile glycerol at –80°C. At the beginning of each round of adaptation, the parental and evolved strain were recovered from the frozen stocks and streaked on a fresh glucose (or xylose) plate containing yeast extract and peptone (YP) as nutrient sources before inoculation to enable visual inspection of colony morphology and ensure that any differences in performance was the result from adaptation to the specific

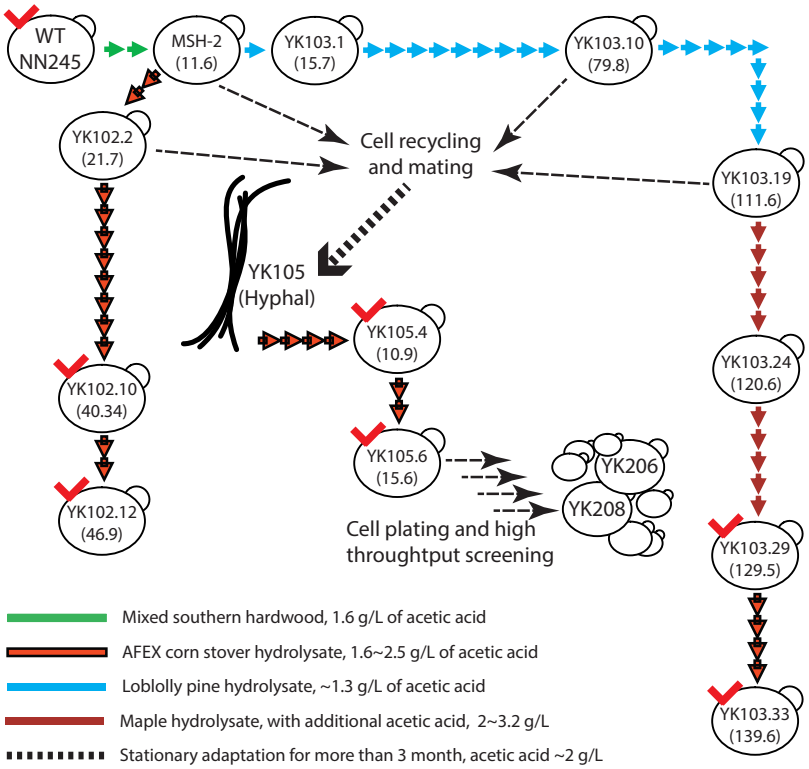

Figure 1. A lineage map of adapting *S. passalidarum* in this study. The number under the strain ID with () indicates the numbes of total generations. Strains with check mark indicate the stains were selected for benchmark 1.

Table 1. A summary of adapted *S. passalidarum* strains used in this study.

Adapted strain[a]	Hydrolysate used[b]	Description
YK102.10 (40.34)	MSH→AFCS	Wild-type (WT) strain adapted in MSH for 2 passages (MSH-2), then in AFCS for 10 passages
YK102.12 (46.9)	MSH→AFCS	Wild-type (WT) strain adapted in MSH for 2 passages (MSH-2), then in AFCS for 12 passages
YK103.29 (129.5)	MSH → LP → MA	Wild-type (WT) strain adapted in MSH for 2 passages (MSH-2), then cultivated in LP hydrolysate for 19 passages (YK103.19) and then in MA hydrolysate for 10 passages
YK103.33 (139.6)	MSH → LP → MA →AFCS	Wild-type (WT) adapted in MSH for 2 passages (MSH-2), then cultivated in LP hydrolysate for 19 passages (YK103.19) and then in MA hydrolysate for 10 passages. After then, the culture (YK103.29) is cultivated in AFCS hydrolysate for four passages
YK105	AFCS	Recycling and mated MSH-2, YK102.2, YK103.10 and YK103.19. The mixed culture were cultivated in AFCS hydrolysate stationarily for more than 3 months
YK105.4 (10.9)	AFCS	YK105 adapted in AFCS hydrolysate for four passages
YK105.6 (15.6)	AFCS	YK105 adapted in AFCS hydrolysate for six passages
YK206-D11	AFCS	Selected from high-throughput screening of YK105.6 population and cultivated in AFCS hydrolysate for three passages
YK206-F2	AFCS	Selected from high-throughput screening of YK105.6 population and cultivated in AFCS hydrolysate for three passages
YK208-E11	AFCS	Selected from high-throughput screening of YK105.6 population and cultivated in AFCS hydrolysate for three passages

The number in () indicates the numbers of generation during the adaptation process; one generation equals to one doubling.
MA, maple hydrolysate; MSH, mixed southern hardwood hydrolysate; LP, loblolly pine hydrolysate; AFCS, AFEX corn stover hydrolysate

hydrolysate used. Figure 1 presents the adaptation process used in this study, and a detailed list of adapted strains with description is shown in Table 1. Wild-type NN245 was first adapted to mixed southern hardwood for two passages to obtain MSH-2 (11.6 generations), and MSH-2 was adapted with two different routes to obtain two descendent strains YK102.12 (12 passages, 46.9 generations) and YK103.33 (33 passages, 139.6 generations).

YK105 was obtained by co-culturing four different adapted strains (MSH-2, YK102.2, YK103.10 and YK103.19) in AFEX-pretreated corn stover (AFCS) hydrolysate medium. These four strains were obtained following serial subculture in (i) mixed southern hardwood hydrolysate, (ii) loblolly pine hydrolysate, (iii) maple hydrolysate with additional acetic acid and (iv) AFCS hydrolysate. Following batch adaptations to the four hydrolysates in shake flasks individually, about 40 ml of cell suspensions from MSH-2, YK102.2, YK103.10 and YK103.19 were combined into a 500-ml flask containing 150 ml of AFCS hydrolysate. The final volume of the mixed culture was

≈300 ml. This mixed culture was maintained at 30°C without shaking for more than 3 months to avoid excess aeration into the system. Stationary incubation was used to select adapted strains capable of growing under very limited oxygen. Plating on synthetic minimal medium plus xylose (ScX) was used periodically to test cell viability. Plating on YPD agar and microscopic inspection were used periodically to check for possible contamination during adaption. During this adaption process, the hydrolysate was supplemented with urea, phosphate buffer, trace metal and vitamin solutions as previously described (Long *et al.* 2012).

The second batch adaptation was carried out with candidate strains selected from high-throughput screening (described below). The preculture was prepared by transferring loopfuls of YK206-D11, YK206-F2 and YK208-E11 (obtained from high-throughput screening) from fresh AFCS plates into HYPX broth in three 125-ml flat-bottom flasks separately and cultured at 30°C, 200 rpm. Appropriate amounts of overnight cultures (OD ≈ 25) were then collected and transferred into 125 ml flasks containing 50 ml of AFCS hydrolysate (pH = 5) to reach an OD of ∼5. The adaptation was performed at 100 rpm, 30°C. The 100 rpm was chosen because we are more interested in mutant strain that can detoxify hydrolysate under low aeration conditions.

Daily sampling (0.8 ml) was withdrawn to monitor cell density and extracellular metabolites. Cells were directly transferred to subsequent shake flasks when the maximum ethanol concentration was attained, which usually occurred in about 6 to 7 days. One per cent (v/v) YP (100 μL of 5× YP), which had a final concentration of 0.01 g/L yeast extract and 0.02 g/L peptone, was supplied in the subsequent flasks (50 ml) to provide enough mineral and vitamins for cell division and detoxification of AFCS hydrolysate during adaptation.

Hydrolysate preparation and hydrolysate plates

Mixed southern hardwood, maple and loblolly pine hydrolysates were generously provided by SUNY-ESF (Syracuse, NY). Mixed southern hardwood and maple hydrolysates were prepared with hot water extraction followed by dilute acid hydrolysis and two-stage membrane filtration (Hu *et al.* 2010). Loblolly pine hydrolysate was prepared by pretreating with oxalic acid (Li *et al.* 2011). AFCS was kindly provided by DOE Great Lakes Bioenergy Research Center (Madison, WI) and was prepared as described previously (Jin *et al.* 2013). The final AFCS hydrolysate contains around 60 g/L of glucose and 30 g/L of xylose with a final pH of 4.8.

To shorten the time for high-throughput screening to be <48 h, the acetic acid in AFCS hydrolysate was removed with the combination of reverse osmosis and diafiltration (AFCS-RO) by using the similar method described by Lee *et al.* (2011). The acetic acid concentration in AFCS-RO was ≈0.9 g/L. AFCS hydrolysate plate was used to obtain individual colonies for high-throughput screening. AFCS hydrolysate plate contained 50% (v/v) of AFCS hydrolysate with 2% agar.

MEDIA

YPD or YPX agar contained (g/L) glucose or xylose, 20; agar, 20; yeast extract, 10; and peptone, 20. YPD (4%) and YPX (4%) liquid broths were prepared by adding appropriate amounts of autoclaved 40% of glucose (dextrose) or xylose solution to the final glucose (or xylose) at 40 g/L. Since the inoculation in high-throughput screening was performed by directly transferring cultures from a 96-well deep block, to avoid the excess amount of nutrients in the initial growth phase during high-throughput screening in AFCS-RO hydrolysate, YPX (4% xylose) with half amount of yeast extract and peptone (HYPX) was used. 5x YP contains yeast extract, 50 g/L; peptone, 100 g/L. Synthetic (Sc) minimal liquid broth contains a final concentration of 6.7 g/L of yeast nitrogen base with either 20 g/L of glucose (ScD) or 20 g/L of xylose (ScX). For Sc medium agar plates, a final concentration of 2% agar was used.

For tetrazolium agar, a 50x stock solution of 2,3,5-triphenyl-2H-tetrazolium chloride was prepared by dissolving 2.5 g of TTC in 50 ml double distilled water and filter sterilized. A 1.5% agar containing 0.1% TTC, 20 g/L of glucose (or xylose) and 50 mM phosphate buffer (pH 7) was used for overlaying (Ogur, John and Nagai 1957). Stock solutions (50×) of respiration inhibitors were prepared individually at the following concentrations and filter sterilized: ROT, 50 mM; AA, 5 mM; KCN, 5M, and SHAM, 1.3 M. Prior to plating, respiration inhibitors were diluted to following concentrations: ROT, 5 mM; AA, 0.5 mM; KCN, 0.5 M; SHAM, 0.2 M, respectively, and 75 μL of each respiration inhibitor was applied on the plate. By assuming the volume for the respiration inhibitor to diffuse was about 5 ml, the final concentrations of each respiration applied in this experiment on each plate would be ROT, 75 μM; AA, 7.5 μM; KCN, 7.5 mM; SHAM, 3 mM. All media and reagents were sterilized prior experiments.

High-throughput screening of adapted population

We used high-throughput screening to select possible candidates from the adapted population YK105.6. Cells of YK105.6 from shake flask benchmark 1 were plated on five AFCS hydrolysate plates, which yielded 10 to 20 single isolated colonies on each plate. About 12 isolated colonies from each AFCS hydrolysate plate were selected yielding a total of 58 isolated colonies, which were transferred into a 96-deep well block (NUNC) containing 500 μL of liquid broth from row B to G and row 2 to 11. Wells B6 and G11 were not inoculated as they served as checks for contamination and the outer wells (row A and H, column 1 to 12) were filled with 500 μl of sterile H_2O to control evaporation. The deep well block was then sealed with breathable tape (Axygen) and incubated at 30°C, 225 rpm. After 48 h, 10 μl of cell suspension from wells B2 to G11 in the deep well block were directly transferred into a standard 96-well plate (NUNC) with a lid cover containing 190 μL of AFCS-RO in each well from row B to G and column 2 to 11. Wells B6 and G11 were not inoculated and the outer wells were filled with sterile water for evaporation control. The inoculated 96-well plates were placed in a Tecan F500 or M1000 multimode plate reader. The plates were shaken for 2 min out of every 10 with an amplitude of 2 mm. Cell density was measured for 24 to 48 h at 595 nm immediately following each 2-min shaking. Seven rounds of screening with AFCS-RO and one control screening with 4% YPX were carried out to confirm the screening result. Both the fermentation profile (i.e. ethanol concentration and sugar utilization) of the starter cultures and the growth profile by either plotting the data by Excel 2011 or using an automated analysis (GCAT, http://gcat-pub.glbrc.org/) were used. Promising candidate strains were streaked on AFCS hydrolysate plates and incubated at 30°C for maintenance. Glycerol stocks were also prepared by transferring 100 μL of cell suspension from 48-h grown 96-well deep plate into 96-well plates containing 100 μL of 2% YPD (yeast extract, 10 g/L; peptone, 20 g/L; dextrose, 20 g/L) supplemented

with 30% v/v glycerol. The glycerol stock plates were stored at –80°C.

Shake flask benchmarking

Two shake flask screenings were performed in this study. The first compared the abilities of adapted populations to ferment AFCS hydrolysate into ethanol. These adapted populations had been adapted to different hydrolysates over various durations (Table 1). The second experiment was conducted with adapted strains YK206-D11, YK206-F2 and YK208-E11, which were selected from high-throughput screening of the YK105.6 population and adapted with AFCS hydrolysate for an additional 1 month. Cells were grown on 4% YPX overnight (OD = 30) and pelleted at 3000 rpm for 3 min. The cell pellet was then suspended in sterile H_2O and inoculated into a 125-ml Erlenmeyer containing 50 ml of AFCS hydrolysate. The initial OD for benchmark 1 and 2 was 7 and 3, respectively, which corresponds to ≈ 1 and 0.4 g CDW/L. For the first benchmark, nutrients such as nitrogen, mineral solution and vitamins with concentrations mentioned previously were used in the first benchmark as described (Long *et al.* 2012) with an initial pH of 5. For the second benchmark experiment, to avoid excess nutrient, 100 μL of 5x YP, which gave a final concentration of 1% (v/v) YP, was provided. The initial pH was increased to 6. For benchmark 1 and 2, 110 rpm and 90 rpm were used respectively. Samples (0.8 ml) were withdrawn daily to monitor cell density and extracellular metabolites.

Analysis of metabolites and cell dry weight

Cell optical density was measured with an Agilent 8453 spectrophotometer at 600 nm (OD_{600}). To determine yeast cell dry weight (CDW) during hydrolysate fermentation, cells growing in AFCS hydrolysate (2–10 ml) were collected and filtered through a 0.2-μm membrane based on the protocol developed by Postma *et al.* (1989). One OD unit = 0.1416 g CDW/L in hydrolysate. For the aerobic growth experiment with YP medium, 1 OD unit = 0.16 g CDW/L. Extracellular metabolites including arabitol, xylitol, ribitol and glycerol were determined by high-performance liquid chromatography using the method described previously (Su *et al.* 2015).

Yeast growth assay

To compare the growth rate in the presence of lignotoxin (LT), a yeast growth assay on solid medium based on previous publications (Jin *et al.* 2002; Chae *et al.* 2003) was executed with YK206-D11, YK206-F2, YK208-E11 and parental strain NN245 on ScD, ScX and ScX supplied with LT, which was phenolic compounds extracted from AFEX hydrolysate. The LT was kindly provided by Dr Yaoping Zhang at the DOE Great Lakes Bioerergy Research Center (Madison, WI, USA). Cells were cultured overnight with 2% YPD or 2% YPX at 200 rpm, 30°C to an optical density (OD_{600}) of at least 1.0. Four 1:10 serial dilutions were prepared, and 3 μL of cell suspension (3 μL) from each dilution was spotted on each plate with the initial OD_{600} of 0.2 on each plate. The plates were incubated at 30°C until the colonies can be visualized.

Tetrazolium overlay with respiration inhibitors

For the tetrazolium overlay, wild-type NN245 and adapted E11 yeast cells grown in ScD broth were plated on ScD agar, and inocula cultured on ScX broth were plated on ScX agar. To insure the cells used for plating were in vigorous aerobic growth phase, a two-stage inoculation preparation was used. A small seed inoculum was cultured in tilted (45°) culture tubes containing 3 ml of ScD broth shaking at 225 rpm, 30°C for 6–8 h. Then, adequate amounts of each cell suspension was transferred into 125-ml Erlenmeyer flasks containing 25 ml of ScD to reach an initial OD_{600} of 0.005 and flasks were incubated with shaking at 225 rpm, 30°C. Cells were collected for plating when the culture is in the active log phase (OD_{600} between 0.8 and 2). Respiration inhibitors (75 μL) were spread onto the surfaces of ScD plates. After the plates dried, 90 μL of yeast cells with an OD_{600} of 2×10^{-5} was plated onto each ScD plate, which yielded ~200 colonies on a control plate without respiration inhibitors. The ScD plates were incubated at 30°C until colonies had developed (2–6 days). Each plate was then gently overlaid with tetrazolium agar. Prior to overlaying, the tetrazolium agar was maintained at 45°C. Fresh plates (held not more than 4 days at 4°C since plating) were used for the tetrazolium overlay experiment. After overlaying, the plates were incubated at 30°C for 12 h (Trevors 1982). Five different conditions were tested on both strains separately, which included overlaying with each of respiration inhibitors: ROT, AA, KCN and the combination of AA plus SHAM (AASH). No inhibitor was added to the control plate. An experiment with ScX plates was also performed with the identical protocol mentioned here.

The results were documented by scanning at 300 dpi each plate with an EPSON v350 scanner and analyzed using Adobe Photoshop CS5. The colony diameter was calculated based on the relationship between the diameter of a Petri dish (in mm) and the pixel measurement on the computer (85 mm = 2025 pixels). Duplicate plates were performed in each condition, and 40 colonies from each plate were measured, which results in n = 80. RStudio 1.1.419 (R version 3.3.3) with Student's *t*-test was used for the statistical analysis of the colonies diameter. A flowchart of the tetrazolium overlay procedure is presented in Fig. S1 (Supporting Information).

Genome sequencing, assembly and annotation

To confirm that all the mutant strains after the adaptation process were still *S. passalidarum*, D1/D2 sequences of large subunit (26S) of ribosomal DNA of all evolved strains (Table 1) were performed (Kurtzman and Robnett 1998). Later, we extracted genomic DNA from strain YK208-E11 and subjected the material to whole genome sequencing following the earlier work (Riley *et al.* 2016) with at least ×40 coverage. The genome assembly was done with Geneious R10 plus Bowtie2 plugin (Kearse *et al.* 2012; Langmead and Salzberg 2012). The parental wild-type NN245 was used as a reference genome downloaded from Joint Genome Institute (https://jgi.doe.gov/). Gene annotation was done first by JGI automatic pipeline (Wohlbach *et al.* 2011) and then manually curated.

RESULTS

Evolved hyphal strain YK105 and the first benchmark

We hypothesized that growth in AFCS hydrolysate under a highly oxygen-limited environment could select for adapted cells able to ferment this hydrolysate. Since we had already adapted various strains (MSH-2, YK102.2, YK103.10 and YK103.19) to hydrolysates containing many of the same inhibitors by culturing them on different hydrolysates (Table 1), we decided to mix these cultures, transfer them into a stationary

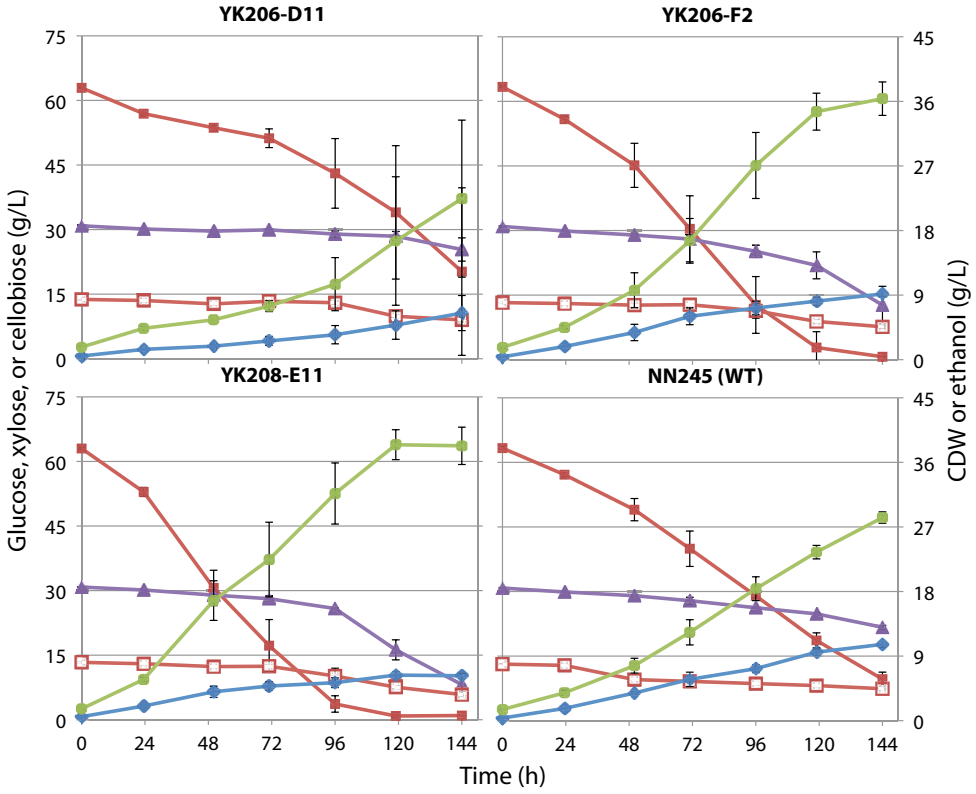

Figure 2. Fermentation of AFCS hydrolysate in shake flasks by adapted *S. passalidarum* YK206-D11, YK206-F2, YK208-E11 and parental WT strain NN245. Symbols: red filled squares, glucose; purple filled triangles, xylose; red open squares, cellobiose; green filled circles, ethanol; blue filled diamonds, cell dry weight. Error bars indicate the standard deviation from triplicate shake flask.

flask containing AFCS hydrolysate (6% glucose, 3% xylose) and keep it at 30°C for more than 3 months. The limited nutritional and aeration conditions induced mating as evidenced by the microscopic observation of asci. After 3 months of adaptation in a no-shaking (stationary) flask, the mixed culture was streaked on both YPX and YPD plates. Interestingly, the isolated colonies formed a rough surface on both YPD and YPX plates. Further inspection under the microscope showed that the most abundant cell morphologies (~95%) from YPX plates had hyphal structures rather than the yeast or pseudomycelial forms previously observed. Both pseudomycelial cells and hyphal structures were found from cells cultivated on YPD or YPX plates. The hyphal cells were much thinner and more elongated as compared to the pseudomycelial cells from the adapted strain YK102.10 (Fig. S2, Supporting Information). A single colony from the YPX plates was streaked three successive times on the same medium to determine whether its hyphal morphology would revert to a yeast-like phase, but it did not. The hyphal strain was named YK105. The D1/D2 sequencing result of YK105 showed that this segment was identical to the parental *S. passalidarum*, NN245. Later, YK105 was subjected to repetitive batch adaptation in AFCS hydrolysate by subculturing six times in shake flasks, and both strains YK105.4 (after four rounds of subculture) and YK105.6 (after six rounds) were compared with the other adapted strains from various rounds of adaptation. The results showed that, after this long period of fermentation (10 days), only YK105.4, YK105.6 and NN245 (wild type) were able to consume both glucose and xylose and produce ethanol from the hydrolysate (Fig. S3, Supporting Information). This result indicates that many of the cell lines had lost desired traits during the adaptation process.

Adaptation and benchmarking of selected strains from high-throughput screening

Because we adapted YK105.6 by transferring a portion of the culture into subsequent flasks without picking single isolated colonies from plates, it was assumed to be a heterogeneous population in which some cells could have substantially better fermentation potential than others. To test this, we isolated 58 colonies from the YK105.6 adapted population by cultivation on AFCS hydrolysate plates, and subjected them to seven rounds of high-throughput screening in 96-well plates with AFCS hydrolysate that had been treated with reverse osmosis (AFCS-RO) to remove low-molecular-weight inhibitors. Three potential candidates (YK206-D11, YK206-F2 and E11) were identified based on it ethanol concentration and sugar utilization during the inoculum preparation prior to the high-throughput screening and their growth rates during the screening. These strains were adapted to AFCS hydrolysate for one additional month (Fig. S4, Supporting Information). During adaptation, the culture was transferred every 6 to 7 days. Analyses of the supernatant solutions showed an average ethanol yield of 0.443 g/g and cell yield of 0.065 g/g. The average ethanol productivity during the adaptation period was 0.197 g/L · h. A triplicate shake flask experiment was performed to compare YK206-D11, YK206-F2 and E11 with the parental strain NN245 in AFCS hydrolysate (Fig. 2).

Both adapted strains and parental NN245 exhibited the potential to co-utilize glucose, xylose and cellobiose for ethanol production. Both E11 and YK206-F2 consumed most of the glucose (>95%) in 4–5 days and utilized about two-thirds of the xylose in 6 days, while the NN245 strain converted about 85% of the glucose but used less than one-third of the xylose in

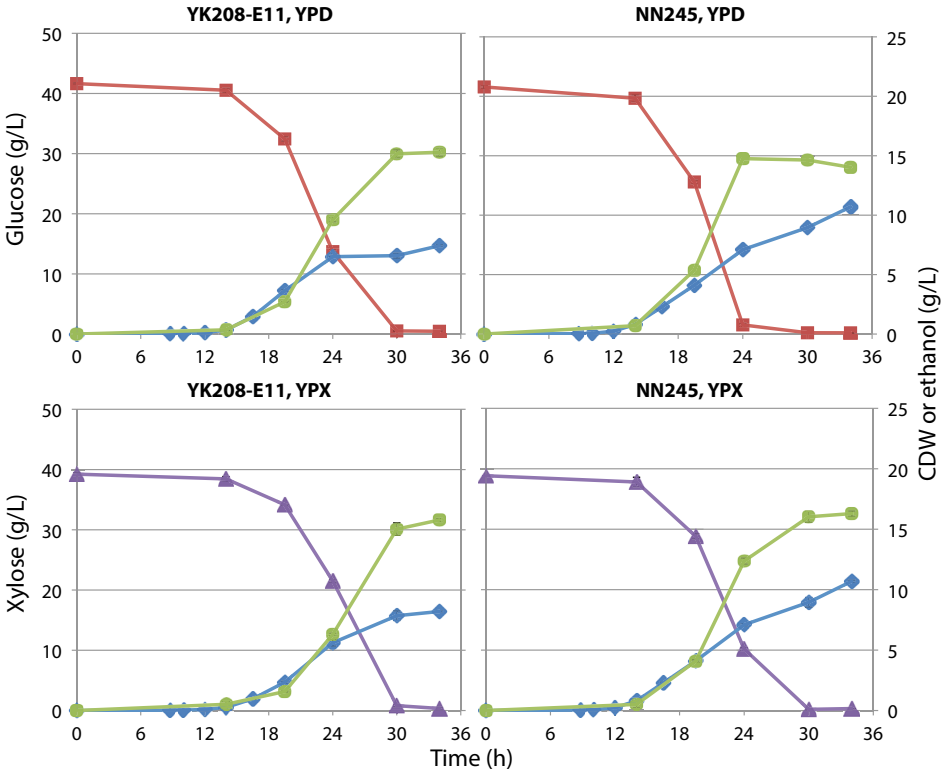

Figure 3. Growth of *S. passalidarum* NN245 and adapted strain YK208-E11 with 50 ml of 4% YPD or 4% YPX in triplicate 125-ml shake flasks under aerobic condition (200 rpm). Symbols: red squares, glucose; purple traingles, xylose; blue diamonds, cell dry weight. Error bars indicate the standard deviation from triplicate shake flask.

6 days. YK206-D11 was unstable and had a slower average sugar utilization and fermentation rate compared to parental NN245. Among the three adapted strains, E11 stood out due to its shorter lag phase for glucose consumption compared to YK206-F2 and reached its peak ethanol (38.3 g/L) at 120 h. The ethanol productivity of E11 was 0.309 g/L · h, which was 1.6 times higher than that of the NN245 strain (0.186 g/L · h). By comparing CDW, we found that the E11 accumulated only about half as much cell mass compared to the NN245 strain, and E11's specific ethanol productivity was 0.05 g/g CDW h, or about three times higher than that from NN245 strain (0.017 g/g CDW h).

Co-utilization of cellobiose (35%–56% of consumption) was also observed during the experiment. The ethanol yield of E11 was 0.48 g/g when excluding the cellobiose uptake and was 0.445 g/g when including cellobiose consumption. We also compared consumption of acetic acid and formation of fermentation by-products (Fig. S5, Supporting Information). Interestingly, YK206-F2 and parental NN245 showed faster acetic acid degradation compared to YK206-D11 and E11. Xylitol accumulation was negligible for NN245 and YK206-D11; E11 accumulated more xylitol, glycerol and arabitol than the other three strains (Fig. S5, Supporting Information).

Characterization of E11 physiology

To further compare the E11 cell yield and growth rate with the NN245 strain, a yeast growth assay was conducted with YK206-D11, YK206-E11, E11 and the parental NN245 on ScD, ScX and ScX plus LT (Fig. S6, Supporting Information). Strain E11 grew slowly on all three media compared to the other strains, as determined by the relative diameters of microcolonies. We then examined both E11 and NN245 in either 4% YPX or 4% YPD broth under aerobic conditions (200 rpm) in triplicate shake flasks. The inocula were prepared by cultivating yeast cells in either 4% YPX or YPD overnight and directly transferred into medium with corresponding carbon source (glucose-grown starters for glucose flasks and xylose-grown starter for xylose flasks) with cultures having an initial OD_{600} of 0.005. Under these conditions, E11 showed less cell yield than NN245 (Fig. 3). The difference was especially apparent when glucose was the carbon source. In that case, the cell yield of E11 was about 66% of the NN245 yield. When xylose was the carbon source, the E11 cell yield was about 77% of the NN245.

Tetrazolium overlay with respiration inhibitors

To investigate whether the adapted strains had acquired any mutations in the ETC, we plated cells on ScD and ScX agar containing respiration inhibitors. We assessed the presence of mutations in three ways: (i) by determining the number of viable colonies formed under each condition when plating from fresh cell suspensions, (ii) by assessing the growth rates of colonies and (iii) by determining the intensity of the tetrazolium reactions following overlay.

Cell viability

Fresh cell suspensions were plated onto ScD or ScX as cell viability controls to determine whether fewer colonies were formed in the presence of respiration inhibitors (Table S1, Supporting Information). When plating NN245 or E11 cells on ScD or ScX in the presence of KCN or ROT, we found similar numbers of colonies on control and test plates. However, only about 50% of the NN245 cells were viable when plated on ScD with AA plus

salicylhydroxamic acid (AA + SH) and only 10% were viable when the carbon source was xylose (ScX). For E11, about half of colonies grew on ScD with AA + SH, which was similar to what has been observed with NN245, but no colony grew out on ScX with AA + SH within 7 days.

Growth rates

Growth rates were determined by (i) how fast the colonies attained the average minimum diameter (>0.5 mm) for the TTC overlay, and (ii) the average of colony diameters after the TTC overlay. After viable colonies had grown out sufficiently, we overlaid the surface of the plate with agar containing 0.1% TTC. For control plates and plates containing KCN, incubation of E11 and NN245 for 48 h was sufficient for ScD or ScX plates (Table S1, Supporting Information). When ROT was present, at least 72 h incubation time was required for E11 for the TTC overlay, while NN245 needed only 48 h. Either strain on ScD or ScX plates containing AA + SHAM required at least 5 days for colony development. For E11, no colonies were observed after 7 days on ScX with AA + SH.

For NN245 with glucose, applying AA + SHAM significantly reduced its colony diameters ($P < 0.001$) compared to those on ScD (Fig. 4A). E11 showed relatively similar colony diameters when glucose is the carbon source except for the plates with AA + SH, which reduced E11's average colony diameter to 65% (0.56 mm) compared to the ScD plate. When switched to xylose from glucose (Fig. 4B), NN245 with AA only and with AA + SH showed a 50% smaller colony diameter (0.94–0.72 mm) compared to other conditions. Similarly, E11 cells growing on ScX with AA had colony diameters 50% smaller compared to the colony diameter from control plates without AA. Interestingly, no colony of E11 was found from ScX with AA + SH.

In general, E11 showed smaller colonies and slower growth rates compared to NN245 among all the conditions test here. When cells grew on ScD plus KCN (48-h growth), colony diameters of E11 were about 73% of the NN245 strain. When xylose was the carbon source and KCN was added, the colony diameters of E11 were about 62% of the NN245 strain (Fig. 4B). On plates with AA, the colony diameters of both NN245 and E11 were significantly smaller with xylose than with glucose as the carbon source. Surprisingly, NN245 showed bigger colonies on ScX with ROT or KCN than it did on control plates in the absence of these inhibitors.

Tetrazolium reaction

Differences in colony colors after TTC overlay were also observed (Fig. 5). Surprisingly, when glucose was the carbon source, E11 colonies showed exclusively dark red, while the colonies of NN245 could be red, pink, a pink circumference with a red center or a light center with a pink circumference depending on the respiration inhibitors. When ScX plates were used, both E11 and NN245 had lighter tetrazolium reactions on xylose than they did on glucose. Pink, faint pink or white colonies were observed under most circumstances except for E11 cultivated without any inhibitors, which exhibited red colonies. Also, E11 exhibited darker color compared to NN245 strain mostly with the same tested condition except with xylose plus KCN. When comparing the colonies of the NN245 on ScD and ScX in the presence and absence of KCN, which blocks the terminal oxidation step by inhibiting the transfer of electrons from cyt c to cytochrome oxidase (aa_3), the colonies on ScX plus KCN did not show a distinct dark center on xylose control plates. ROT

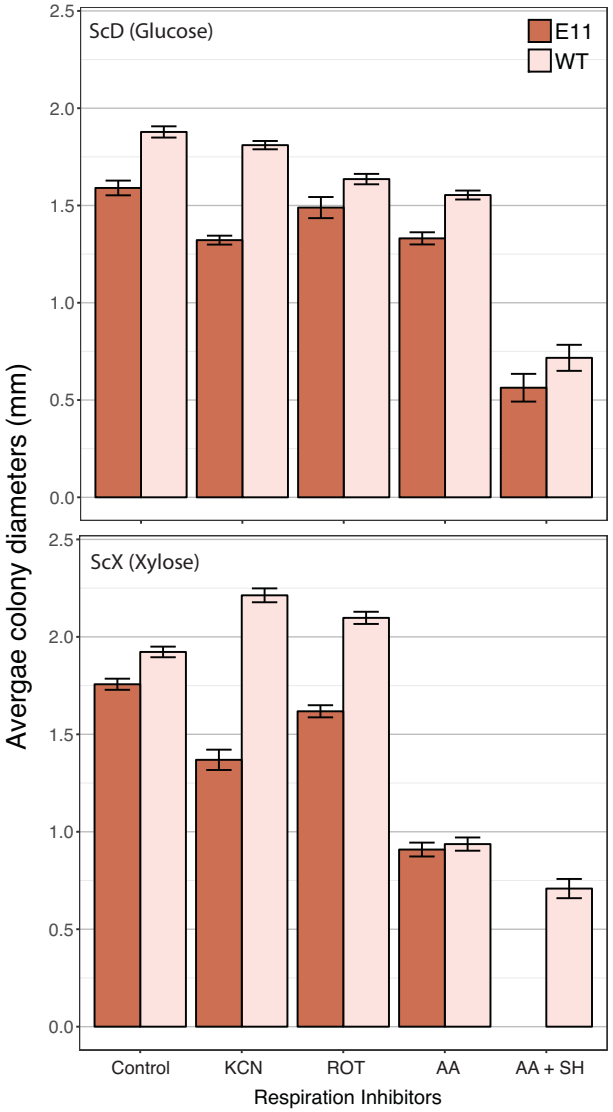

Figure 4. Average colony diameters with 95% confidence interval (n = 80) of *S. passalidarum* NN245 and YK208-E11 (E11) on ScD (**A**) or ScX (**B**) plates containing respiration inhibitors and overlaying with tetrazolium (0.1%) agar. Inhibitor concentration used for plating: ROT, 50 mM; AA, 0.5 mM; KCN, 0.5 M; SHAM, 0.2 M; AASH, AA + SHAM. Plating volume: 75 μL for the inhibitor and 90 μL of cell suspension ($OD_{600} = 2 \times 10^{-5}$).

appears to repress respiration (colony color turns white pink) without greatly restricting cell growth on xylose, especially for NN245. The NN245 strain appeared white when growing on ScX plus AA or ScX with AA + SH, and in the latter condition, colonies only grew near the edge of the petri dish where oxygen availability was highest (Fig. 5P and T).

Genome sequencing of mutant strain YK208-E11

The E11 genome was sequenced with an average of ×64 coverage. The genome size of E11 was ≈ 13.2 Mbps with 37.4% GC content, which was very similar to what was previously reported for its parental wild-type (Wohlbach *et al.* 2011). In scaffold 2, we identified a region of ~11 kb near the potential centromere location that is present in strain NN245 but deleted in E11 (Fig. S7, Supporting Information). This genetic region

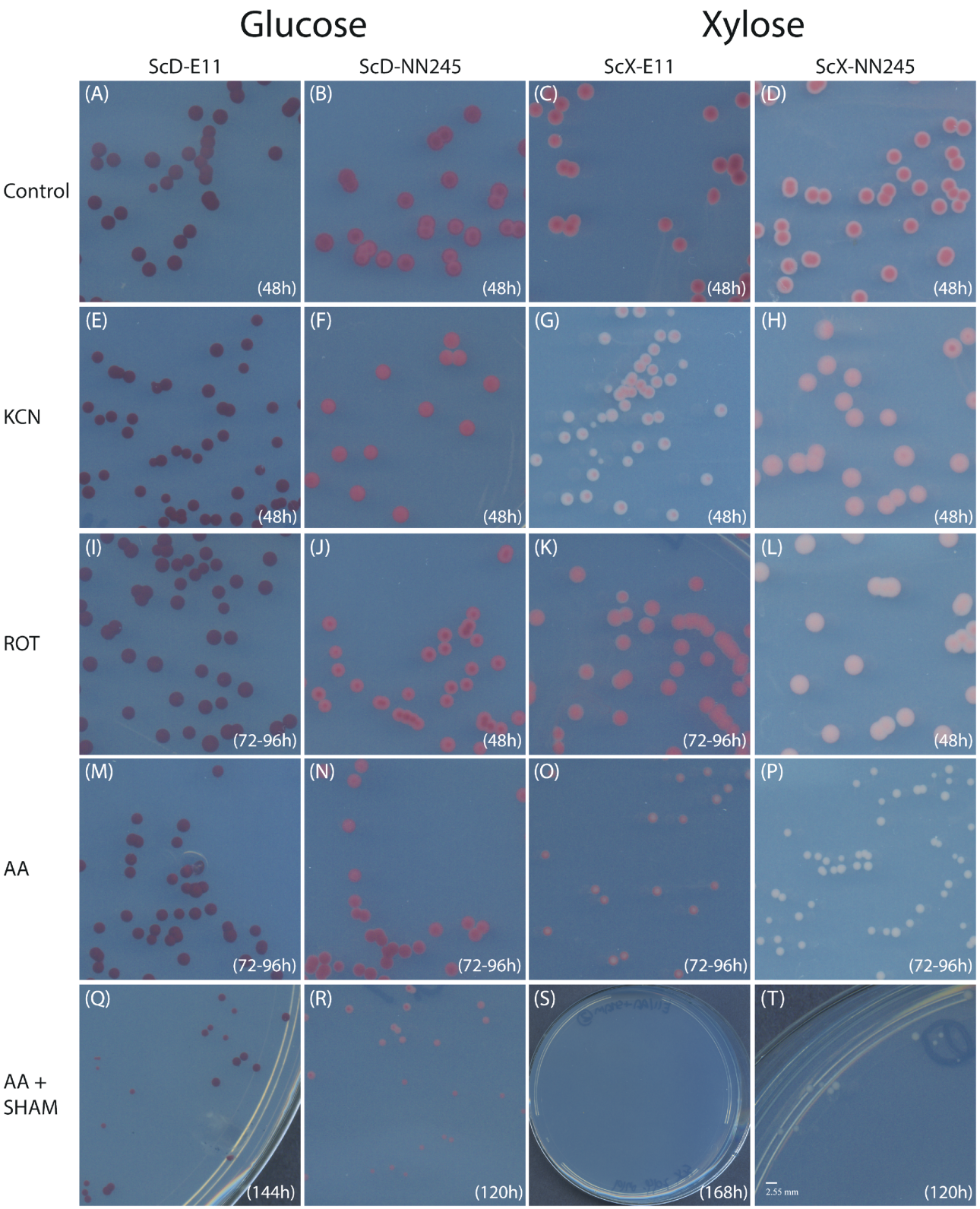

Figure 5. Comparison of *S. passalidarum* YK208-E11 and parental WT strain NN245 on either ScD or ScX plate overlaying with tetrazolium (0.1%) with respiration inhibitors. Inhibitor concentration used for plating: ROT, 50 mM; AA, 0.5 mM; KCN, 0.5 M; SHAM, 0.2 M. Plating volume: 75 μL for the inhibitor and 90 μL of cell suspension ($OD_{600} = 2 \times 10^{-5}$). Control (no inhibitors): (A) to (D); with KCN: (E) to (H); with ROT: (I) to (L); with AA: (M) to (P); with AA+SHAM: (Q) to (T).

Table 2. Annotated proteins in the deleted region of Scaffold 2 that have possible relationships to observed physiology of the mutant strain YK208-E11.

Protein Id	Start	End	Strand	Automated annotations	User Annotations	Function
48889	217268	219571	(–)	GO:0000166 GO:0005524 GO:0017111 KOG:KOG0740 KEGGEC:ec:3.6.1.3 IPRF:ipr003593 IPRF:ipr003959 IPRF:ipr003960 IPRF:ipr015415 PFD:pf00004 PFD:pf09336	3′: Partial identity to AAA ± type ATPase; CDC48; 5′: DUF4045:	Cell division cycle
70049	224916	227012	(+)	KOG:KOG3671 IPRF:ipr000697 IPRF:ipr003124 PFD:pf00568 PFD:pf02205	Actin regulatory protein (Wiskott-Aldrich syndrome protein)	Actin-related
70066	267158	270047	(–)	GO:0005507 GO:0005743 GO:0006118 GO:0006825 GO:0006878 GO:0008535 KOG:KOG2792 IPRF:ipr003782 IPRF:ipr012336 IPRF:ipr017276 PFD:pf02630	Putative cytochrome C oxidase assembly protein	Respiration
59159	278194	279896	(+)	KOG:KOG0642 KEGGEC:ec:3.6.1.3 IPRF:ipr013258 PFD:pf08232	Cell-cycle nuclear protein, contains WD-40 repeats	Cell cycle
48919	280268	283879	(+)	GO:0000166 GO:0000785 GO:0003682 GO:0005488 GO:0005524 GO:0005634 GO:0006333 GO:0016887 GO:0017111 KOG:KOG0062 IPRF:ipr000953 IPRF:ipr003439 IPRF:ipr003593 IPRF:ipr016024 PFD:pf00005 PFD:pf00385	Translation elongation factor EF-3; chromatin binding and assembly; ATPase component of ABC transporters with duplicated ATPase domains	Translation elongation
59166	295081	296126	(+)	GO:0006118 GO:0016491 KOG:KOG0534 KEGGEC:ec:1.6.2.2 IPRF:ipr001433 IPRF:ipr001709 IPRF:ipr001834 IPRF:ipr008333 PFD:pf00175 PFD:pf00970	NADH-cytochrome b-5 reductase	Respiration
59180	314426	315784	(–)	GO:0005515 KOG:KOG0677 IPRF:ipr004000 PFD:pf00022	Actin-related protein Arp2/3 complex, subunit Arp2	Actin-related
134703	390425	392581	(–)	GO:0006270 KOG:KOG2475 IPRF:ipr003874 PFD:pf02724	CDC45 (cell division cycle 45)-like protein	Cell division cycle
59206	399851	401379	(–)	GO:0004497 GO:0006118 GO:0006725 GO:0008152 GO:0016491 KOG:KOG3855 KEGGEC:ec:1.14.13.7 IPRF:ipr002938 IPRF:ipr003042 IPRF:ipr012336 IPRF:ipr012941 PFD:pf01494 PFD:pf07976	Monooxygenase involved in coenzyme Q (ubiquinone) biosynthesis	Respiration
133792	308105	309721	(+)	KOG:KOG3671	Actin regulatory protein (Wiskott-Aldrich syndrome protein)	Actin-related

contains several open reading frames that code for proteins with predicted functions in respiration, cell division and the actin cytoskeleton. Deletion of the respiration-related proteins could be particularly significant in effecting the observed physiology of the adapted strain (Table 2). We also identified a region on scaffold 7 with a potential duplication (Fig. S8, Supporting Information). BLAST analysis of the duplicated region revealed that the sequence is 97% identical to an ATP-dependent multidrug resistance ABC transporter (NCBI access no: XM˙007377498.1). A similar result was also obtained when blasting the region against JGI *S. passalidarum* NRRL Y-27907 v2.0 (https://genome.jgi.doe.gov/Spapa3/Spapa3.home.html). Since the E11 strain had been evolved to increase its tolerance to toxic compounds in hydrolysates, duplication of a region related to a multidrug resistance transporter could contribute to the observed strain phenotype.

DISCUSSION

Batch adaptation and selection for potential fermentative candidates

Batch and continuous culture-based methods have been applied to select for yeasts with improved resistance to acetic acid (Wright *et al.* 2011; Cakar *et al.* 2012; Kim *et al.* 2012; Koppram, Albers and Olsson 2012; Oud *et al.* 2012; Demeke *et al.* 2013; Harner *et al.* 2014). Likewise, numerous strains have been adapted to resist furfural and HMF (Lin, Qiao and Yuan 2009; Tian, Zhu and Yang 2011; Koppram, Albers and Olsson 2012). Recursive selection and adaptation—particularly when it combined with mating between successive rounds of selection, has proven especially effective in obtaining strains of *S. cerevisiae* resistant to hardwood spent sulfite liquor (Pinel *et al.* 2011; den Haan *et al.* 2013; Kim *et al.* 2013; Pereira *et al.* 2013). One reason for the efficacy of this approach could be that in developing resistance to complex mixtures of inhibitors, different yeasts acquire different mutational events, and through recursive mating, the various resistance mechanisms are combined into the most resistant strains. Efficient xylose-fermenting diploid strains of *S. cerevisiae* can also be obtained by mating strains that have been engineered independently (Kim *et al.* 2013). In our experiments, four lines of cells that had been adapted to separate hydrolysates were combined into a single flask and cultivated on AFCS hydrolysate under oxygen-limited (stationary) conditions for 3 months. Microscopic observation of the culture broth indicated that mating occurred during this time.

We hypothesized that using more passages during the batch adaptation in hydrolysates might significantly reduce the

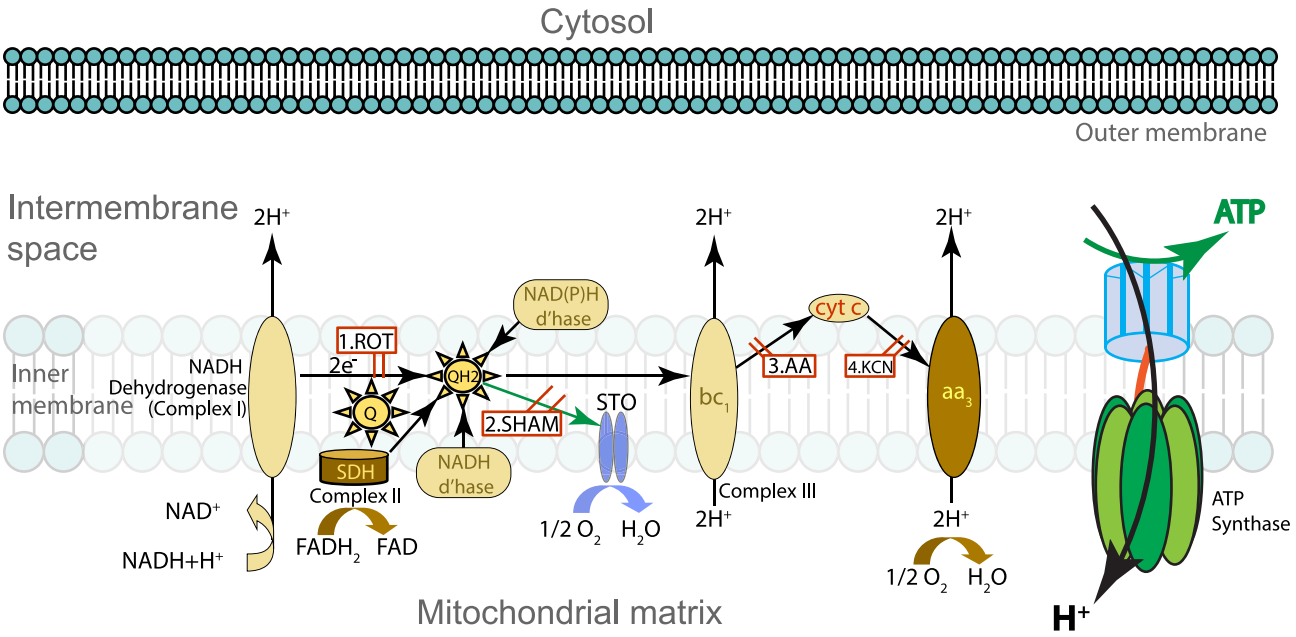

Figure 6. A typical diagram of alternative and standard redox components in the ETC in *S. passalidarum* or *S. stipitis*. The AOX pathway is shown in green arrow and can be block by SHAM. ROT, rotenone; SHAM, salicylhydroxamic acid; AA, antimycin A; NAD(P)H d'hase, retonone-insesitive dehydrogenase; SDH, succinate dehydrogenase; STO, SHAM-sensitive terminal oxidase.

number of cells and strains with fermentative ability because most fermentative growth (as opposed to respiration) generates less ATP and fermentative cells tend to grow slower and produce fewer cells as compared to respiring cells. This presented a paradox: we wanted to select for faster growth on hydrolysate, but we also wanted to select for more fermentative cells, which tended to grow more slowly and to exhibit lower cell yield.

By comparing the cell densities at day 5 (Fig. S2, Supporting Information), we could see that YK102.10 and YK102.12, transferred in AFCS for 10 and 12 passages, respectively, were able to escape from the lag phase faster than YK105.4 and YK105.6. Similar observations were found when comparing YK103.29 and YK103.33 to YK105.4 and YK105.6. These results imply that (i) a population with faster initial growth would be selected during serial transfers in batch adaptation, (ii) this selection could benefit cells that can make more cell mass and (iii) this would put fermentative cells at a disadvantage.

We also exercised the same concept for selecting the promising candidate from AFCS plates. In this case, E11 was selected because of its lesser growth in the 96-well plate and its relative higher ethanol concentration during the inoculum preparation (data not shown). During the second batch adaptation, our data clearly suggested a better fermentative performance of E11 compared to YK206-D11 and YK206-F2.

Cell growth and the colony diameter on ScD or ScX plates containing respiration inhibitors

The consistently lower cell yield of E11 compared to other strains was also confirmed by drop tests and shake flask experiments under aerobic conditions (200 rpm). To investigate the possibility that E11 had a disruption or defect in its mitochondrial ETC, we used ScD or ScX plates in the presence or absence of four different respiration inhibitors overlaid with tetrazolium agar to detect respiratory activity. Figure 6 shows a typical respiratory chain including the action site of each respiration inhibitor in native xylose-fermenting yeasts *S. stipitis*. Based on the observation of colony count (Table S1, Supporting Information) and colony diameters (Fig. 4) from the parental NN245, we infer that the parental *S. passalidarum* NN245 is SHAM-sensitive and KCN-insensitive. Since *S. passalidarum* and *S. stipitis* are evolutionarily closely related, it is not surprising that *S. passalidarum* (like *S. stipitis*) is also cyanide-insensitive and has a SHAM-sensitive alternative oxidase (AOX) pathway (Jeppsson, Alexander and Hahnhagerdal 1995; Shi *et al.* 2002). Studies have also shown that when the cyanide resistance is present in yeast or fungi, and complex I is also present, the presence of AOX pathway is very common in yeast and fungi (Veiga, Arrabaca and Loureiro-Dias 2000; Joseph-Horne, Hollomon and Wood 2001; Veiga *et al.* 2003).

Rosenfeld and Beauvoit (2003) concluded that cyanide-resistant AA-resistant yeasts possess a SHAM-sensitive AOX pathway, which transfers electrons directly from ubiquinol to molecular oxygen when the pathway from bc_1 to *cyt c* is blocked. When cyanide is present, despite the block in the flow of electrons from *cyt c* to aa_3, both complex I and complex III are still functional. However, when both AA and SHAM are present, only complex I is able to transfer the electron through the ETC pathway, and therefore sequentially less ATP would be generated through ATP synthase compared to when only cyanide is present. This can explain why fewer colonies, and colonies with much smaller diameters, were found with AA plus SHAM compared to the condition when only KCN is present. Similar observations of colony numbers and diameters from NN245 and E11 on ScD or ScX with ROT for NN245 and E11 implied that *S. passalidarum* also possesses ROT-insensitive dehydrogenases (Fig. 6).

By comparing the results from NN245 and E11 (Table S1 and Fig. 5), E11 is more sensitive to respiration inhibitors than NN245, especially when both AA and SHAM were present with xylose as the carbon source. The lower cell yield from the shake flask experiment and the higher sensitivity of E11 to respiration inhibitors implied (i) possible deficiencies with ATP production in the mitochondria, (ii) auxotrophy or (iii) limited

biosynthetic capacity for one or more essential metabolites. The second possibility seemed unlikely since E11 could grow on defined minimal Sc medium. The results from viable cell count and colony diameters also suggest that the presence of xylose may affect ATP production, which subsequently leads to cell death for E11 when both AA and SHAM were applied on ScX plates.

Tetrazolium overlaid with ScD or ScX plates containing respiration inhibitors

When evaluating results from the tetrazolium assay, which has been applied to select respiration deficiency in *S. cerevisiae*, a white or faint pink color suggests repression or disruption of the mitochondrial ETC (i.e. petite colony), while dark red indicates respiration positive strains (Trevors 1982; Conconi *et al.* 2000; Barclay *et al.* 2001). Since TTC serves as an indicator for cellular reducing power, and under most conditions this reaction requires NADH (Berridge, Herst and Tan 2005), we interpret that the reduction of tetrazolium, from white to red, is associated with the concentration of NADH from energy production and cellular respiration. Therefore, the darker tetrazolium reaction with glucose compared to xylose suggests that cells growing on glucose exhibit higher respiration than those on xylose (Fig. 5). On the other hand, the lighter tetrazolium reaction (white or pink) of either NN245 or E11 on xylose compared to glucose implies that the presence of xylose could affect the amount of ATP production (or respiration capacity). The tetrazolium reaction on xylose vs glucose suggests higher specific fermentation rate on xylose than on glucose, which supports our earlier finding on preferential fermentation on xylose in *S. passalidarum* (Long *et al.* 2012).

Our findings showed that E11 produces less cell mass than NN245 and thus the specific fermentation rate of E11 is higher compared to the parental NN245. If the lower cell yield of E11 were due to lower respiration, then we would expect to see a lighter color with E11 compared to the NN245 parental strain when both strains are cultivated on glucose (or xylose) under the same condition. Nevertheless, E11 exclusively showed darker color compared to NN245 under all the conditions tested here (Fig. 5).

A possible explanation is that NADH and NADPH, which are required for the reduction of tetrazolium salts, are also required for yeast cells to detoxify aldehyde inhibitors, such as HMF and furfural (Liu 2011; Ask *et al.* 2013). In addition, most of the dye reduction appears to be non-mitochondrial (Berridge, Herst and Tan 2005). Because tetrazolium salts are lipophilic, they can diffuse through the cell membrane and be reduced in the cytosol. It is possible that E11 contains higher levels of NADH or NADPH compared to the NN245 strain, and a darker color from E11 was observed due to a higher capacity to reduce TTC in the cytosol.

The results of the tetrazolium overlay assay would suggest that the respiration, or to be more precise, the reduction of NADH to NAD+, comes from a non-ATP generating pathway—possibly the SHAM-sensitive terminal oxidase (STO) (Shi *et al.* 2002). Our results imply that E11 has lower respiration or disrupted ETC, which results in less ATP production.

Interestingly, even though similar numbers of colonies were observed with the NN245 strain when cultivated on ScD or ScX with ROT or KCN, the colonies of NN245 plated on ScX with ROT or KCN appeared whiter and larger as compared to those from ScD plates (Figs 4 and 5). We infer from these observations that the cultivation on xylose could affect the ETC pathway in NN245—possibly by inducing the activity of the AOX (or STO, Fig. 6), which could subsequently make the xylose-grown NN245 cells more resistant to ROT or KCN. Thus, colonies growing on xylose will accumulate less NADH and the colonies will appear whiter compared to those growing on glucose. For NN245 growing on ScD + ROT, the extra NADH reduces the TTC so the colonies appeared red. When E11 was cultivated on xylose in the presence of AA and SHAM, we hypothesize that the ETC pathway was completely blocked and cells would have to recycle NADH to regenerate NAD + through ROT-resistant dehydrogenases in its mitochondria. However, since no growth was observed with E11 on ScX with AA + SHAM, it implies that the disruption of ETC in E11 is not in the AOX pathway as we earlier assumed but in its ROT-resistant dehydrogenases. This observation can also explain the longer incubation time for E11 compared to parental NN245 cultivated on plates with ROT.

Through a series of experiments adapting *S. passalidarum* to growth and fermentation in the presence of lignocellulosic hydrolysates, coupled with mating and further selection, we identified strain E11 that exhibits a higher specific fermentation rate and lower cell mass than the parental strain. Based on microscopic observations, experiments with tetrazolium reaction in the presence and absence of respiration inhibitors, and whole genome sequencing data, we conclude that this strain has acquired traits that confer resistance to toxins found in hydrolysates while maintaining higher specific fermentation rates on xylose compared to glucose.

SUPPLEMENTARY DATA

Supplementary data are available at *FEMSYR* online.

ACKNOWLEDGEMENTS

We would like to thank the University of Wisconsin Biotechnology Center DNA Sequencing Facility for providing Illumina next-gen sequencing facilities and services. YKS also would like to thank to Dr Chris Calvey for his advice for yeast genome extraction and Dr Yaoping Zhang for providing the lignotoxin. The authors also acknowledge Ellyn Lepinski, Devon Molony and Qian Wu for their excellent technical efforts.

FUNDING

This work was funded in part by the Department of Energy DOE Great Lakes Bioenergy Research Center (DOE Office of Science BER DE-FC02-07ER64494), by a grant from the Heart of Wisconsin (Wisconsin Rapids) to the University of Wisconsin, Madison and by NSF sub-award # 1264861 from Dr Jin Wang at Auburn University to TWJ at the UW-Madison to pay for genome sequencing. TWJ and LBW were supported in part by the United States Department of Agriculture Forest Products Laboratory.

Conflict of interest. YKS and LBW declare that they have no competing interests. TWJ is President of Xylome Corporation, which is developing *Spathaspora passalidarum* for commercial purposes.

REFERENCES

Adeboye PT, Bettiga M, Olsson L. The chemical nature of phenolic compounds determines their toxicity and induces distinct physiological responses in *Saccharomyces cerevisiae* in lignocellulose hydrolysates. *P Natl Acad Sci USA* 2014;**4**: 299–306.

Allen SA, Clark W, McCaffery JM *et al.* Furfural induces reactive oxygen species accumulation and cellular damage in *Saccharomyces cerevisiae*. *Biotechnol Biofuels* 2010;**3**:2.

Almeida JRM, Runquist D, Nogue VSI *et al.* Stress-related challenges in pentose fermentation to ethanol by the yeast *Saccharomyces cerevisiae*. *Biotechnol J* 2011;**6**:286–99.

Ask M, Bettiga M, Mapelli V *et al.* The influence of HMF and furfural on redox-balance and energy-state of xylose-utilizing *Saccharomyces cerevisiae*. *Biotechnol Biofuels* 2013;**6**:13.

Barclay BJ, DeHaan CL, Hennig UGG *et al.* A rapid assay for mitochondrial DNA damage and respiratory chain inhibition in the yeast *Saccharomyces cerevisiae*. *Environ Mol Mutagen* 2001;**38**:153–8.

Berridge MV, Herst PM, Tan AS. Tetrazolium dyes as tools in cell biology: New insights into their cellular reduction. In: El-Gewely MR (ed.) *Biotechnology Annual Review* vol. 11: Elsevier, Malaghan Institute of Medical Research, Wellington, New Zealand, 2005, 127–52.

Cadete RM, Melo MA, Zilli JE *et al.* *Spathaspora brasiliensis* sp. nov., *Spathaspora suhii* sp. nov., *Spathaspora roraimanensis* sp. nov. and *Spathaspora xylofermentans* sp. nov., four novel D- xylose-fermenting yeast species from Brazilian Amazonian forest. *Anton Leeuw Int J G* 2013;**103**:421–31.

Cadete RM, Santos RO, Melo MA *et al.* *Spathaspora arborariae* sp. nov., a D-xylose-fermenting yeast species isolated from rotting wood in Brazil. *FEMS Yeast Res* 2009;**9**:1338–42.

Cakar ZP, Turanli-Yildiz B, Alkim C *et al.* Evolutionary engineering of *Saccharomyces cerevisiae* for improved industrially important properties. *FEMS Yeast Res* 2012;**12**:171–82.

Casey E, Sedlak M, Ho NWY *et al.* Effect of acetic acid and pH on the cofermentation of glucose and xylose to ethanol by a genetically engineered strain of *Saccharomyces cerevisiae*. *FEMS Yeast Res* 2010;**10**:385–93.

Chae H-J, Ke N, Kim H-R *et al.* Evolutionarily conserved cytoprotection provided by Bax Inhibitor-1 homologs from animals, plants, and yeast. *Gene* 2003;**323**:101–13.

Conconi A, Jager-Vottero P, Zhang XY *et al.* Mitotic viability and metabolic competence in UV-irradiated yeast cells. *Mutat Res-DNA Repair* 2000;**459**:55–64.

Demeke MM, Dietz H, Li YY *et al.* Development of a D-xylose fermenting and inhibitor tolerant industrial *Saccharomyces cerevisiae* strain with high performance in lignocellulose hydrolysates using metabolic and evolutionary engineering. *Biotechnol Biofuels* 2013;**6**:24.

den Haan R, Kroukamp H, Mert M *et al.* Engineering *Saccharomyces cerevisiae* for next generation ethanol production. *J Chem Technol Biot* 2013;**88**:983–91.

Harner NK, Bajwa PK, Habash MB *et al.* Mutants of the pentose-fermenting yeast *Pachysolen tannophilus* tolerant to hardwood spent sulfite liquor and acetic acid. *Anton Leeuw Int J G* 2014;**105**:29–43.

Hasunuma T, Sanda T, Yamada R *et al.* Metabolic pathway engineering based on metabolomics confers acetic and formic acid tolerance to a recombinant xylose-fermenting strain of *Saccharomyces cerevisiae*. *Microb Cell Fact* 2011;**10**:2.

Hou X. Anaerobic xylose fermentation by *Spathaspora passalidarum*. *Appl Microbiol Biot* 2012;**94**:205–14.

Hu RF, Lin L, Liu TJ *et al.* Dilute sulfuric acid hydrolysis of sugar maple wood extract at atmospheric pressure. *Bioresource Technol* 2010;**101**:3586–94.

Hughes SR, Gibbons WR, Bang SS *et al.* Random UV-C mutagenesis of *Scheffersomyces* (formerly *Pichia*) *stipitis* NRRL Y-7124 to improve anaerobic growth on lignocellulosic sugars. *J Ind Microbiol Biot* 2012;**39**:163–73.

Jeppsson H, Alexander NJ, Hahnhagerdal B. Existence of cyanide-insensitive respiration in the yeast *Pichia stipitis* and its possible influence on product formation during xylose utilization. *Appl Environ Microb* 1995;**61**:2596–600.

Jin M, Sarks C, Gunawan C *et al.* Phenotypic selection of a wild *Saccharomyces cerevisiae* strain for simultaneous saccharification and co-fermentation of AFEXTM pretreated corn stover. *Biotechnol Biofuels* 2013;**6**:108.

Jin YS, Jones S, Shi NQ *et al.* Molecular cloning of *XYL3* (D-xylulokinase) from *Pichia stipitis* and characterization of its physiological function. *Appl Environ Microb* 2002;**68**:1232–9.

Jonsson LJ, Alriksson B, Nilvebrant NO. Bioconversion of lignocellulose: inhibitors and detoxification. *Biotechnol Biofuels* 2013;**6**:10.

Joseph-Horne T, Hollomon DW, Wood PM. Fungal respiration: a fusion of standard and alternative components. *BBA-Bioenergetics* 2001;**1504**:179–95.

Kearse M, Moir R, Wilson A *et al.* Geneious Basic: an integrated and extendable desktop software platform for the organization and analysis of sequence data. *Bioinformatics* 2012;**28**:1647–9.

Kim IK, Roldao A, Siewers V *et al.* A systems-level approach for metabolic engineering of yeast cell factories. *FEMS Yeast Res* 2012;**12**:228–48.

Kim SR, Lee KS, Kong II *et al.* Construction of an efficient xylose-fermenting diploid *Saccharomyces cerevisiae* strain through mating of two engineered haploid strains capable of xylose assimilation. *J Biotechnol* 2013;**164**:105–11.

Klinke HB, Thomsen AB, Ahring BK. Inhibition of ethanol-producing yeast and bacteria by degradation products produced during pre-treatment of biomass. *Appl Microbiol Biot* 2004;**66**:10–26.

Koppram R, Albers E, Olsson L. Evolutionary engineering strategies to enhance tolerance of xylose utilizing recombinant yeast to inhibitors derived from spruce biomass. *Biotechnol Biofuels* 2012;**5**:32.

Kurtzman CP, Robnett CJ. Identification and phylogeny of ascomycetous yeasts from analysis of nuclear large subunit (26S) ribosomal DNA partial sequences. *Anton Leeuw Int J G* 1998;**73**:331–71.

Langmead B, Salzberg SL. Fast gapped-read alignment with Bowtie 2. *Nat Methods* 2012;**9**:357–9.

Larsson S, Quintana-Sainz A, Reimann A *et al.* Influence of lignocellulose-derived aromatic compounds on oxygen-limited growth and ethanolic fermentation by *Saccharomyces cerevisiae*. *Appl Biochem Biotech* 2000;**84-6**:617–32.

Lee JW, Houtman CJ, Kim HY *et al.* Scale-up study of oxalic acid pretreatment of agricultural lignocellulosic biomass for the production of bioethanol. *Bioresource Technol* 2011;**102**:7451–6.

Li XJ, Cai ZY, Horn E *et al.* Oxalic acid pretreatment of rice straw particles and loblolly pine chips: release of hemicellulosic carbohydrates. *Tappi J* 2011;**10**:41–5.

Lin F-M, Qiao B, Yuan Y-J. Comparative proteomic analysis of tolerance and adaptation of ethanologenic *Saccharomyces cerevisiae* to furfural, a lignocellulosic inhibitory compound. *Appl Environ Microb* 2009;**75**:3765–76.

Liu ZL. Molecular mechanisms of yeast tolerance and in situ detoxification of lignocellulose hydrolysates. *Appl Microbiol Biot* 2011;**90**:809–25.

Long TM, Su Y-K, Headman J *et al.* Cofermentation of glucose, xylose, and cellobiose by the beetle-associated yeast *Spathaspora passalidarum*. *Appl Environ Microb* 2012;**78**:5492–500.

Lopes MR, Morais CG, Kominek J *et al.* Genomic analysis and D-xylose fermentation of three novel *Spathaspora* species: *Spathaspora girioi* sp. nov., *Spathaspora hagerdaliae* f. a., sp. nov., and *Spathaspora gorwiae* f. a., sp. nov. *FEMS Yeast Res* 2016;**16**, DOI: 10.1093/femsyr/fow044.

Mira NP, Teixeira MC, Sa-Correia I. Adaptive response and tolerance to weak acids in *Saccharomyces cerevisiae*: A genome-wide view. *Omics* 2010;**14**:525–40.

Nardi JB, Bee CM, Miller LA *et al.* Communities of microbes that inhabit the changing hindgut landscape of a subsocial beetle. *Arthropod Struct Dev* 2006;**35**:57–68.

Nilsson A, Gorwa-Grauslund MF, Hahn-Hagerdal B *et al.* Cofactor dependence in furan reduction by *Saccharomyces cerevisiae* in fermentation of acid-hydrolyzed lignocellulose. *Appl Environ Microb* 2005;**71**:7866–71.

StOgur M, John R, Nagai S. Tetrazolium overlay technique for population studies of respiration deficiency in yeast. *Science (New York, NY)* 1957;**125**:928–9.

Oud B, van Maris AJA, Daran JM *et al.* Genome-wide analytical approaches for reverse metabolic engineering of industrially relevant phenotypes in yeast. *FEMS Yeast Res* 2012;**12**:183–96.

Palmqvist E, Hahn-Hagerdal B. Fermentation of lignocellulosic hydrolysates. II: inhibitors and mechanisms of inhibition. *Bioresource Technol* 2000;**74**:25–33.

Pereira SR, Portugal-Nunes DJ, Evtuguin DV *et al.* Advances in ethanol production from hardwood spent sulphite liquors. *Process Biochem* 2013;**48**:272–82.

Pinel D, D'Aoust F, del Cardayre SB *et al.* *Saccharomyces cerevisiae* genome shuffling through recursive population mating leads to improved tolerance to spent sulfite liquor. *Appl Environ Microb* 2011;**77**:4736–43.

Postma E, Verduyn C, Scheffers WA *et al.* Enzymic analysis of the crabtree effect in glucose-limited chmostat cultures of *Saccharomyces cerevisiae*. *Appl Environ Microb* 1989;**55**:468–77.

Riley R, Haridas S, Wolfe KH *et al.* Comparative genomics of biotechnologically important yeasts. *P Natl Acad Sci USA* 2016;**113**:9882–7.

Rosenfeld E, Beauvoit B. Role of the non-respiratory pathways in the utilization of molecular oxygen by *Saccharomyces cerevisiae*. *Yeast* 2003;**20**:1115–44.

Shi NQ, Cruz J, Sherman F *et al.* SHAM-sensitive alternative respiration in the xylose-metabolizing yeast *Pichia stipitis*. *Yeast* 2002;**19**:1203–20.

Stoutenburg RM, Perrotta JA, Nakas JP. Overcoming inhibitors in a hemicellulosic hydrolysate: improving fermentability by feedstock detoxification and adaptation of *Pichia stipitis*. *J Ind Microbiol Biot* 2011;**38**:1939–45.

Su Y-K, Willis LB, Jeffries TW. Effects of aeration on growth, ethanol and polyol accumulation by *Spathaspora passalidarum* NRRL Y-27907 and *Scheffersomyces stipitis* NRRL Y-7124. *Biotechnol Bioeng* 2015;**112**:457–69.

Tian S, Zhu JY, Yang XS. Evaluation of an adapted inhibitor-tolerant yeast strain for ethanol production from combined hydrolysate of softwood. *Appl Energy* 2011;**88**:1792–6.

Trevors JT. Tetrazolium reduction in *Saccharomyces cerevisiae*. *Eur J Appl Microbiol* 1982;**15**:172–4.

Urbina H, Blackwell M. Multilocus phylogenetic study of the *Scheffersomyces* yeast clade and characterization of the n-terminal region of xylose reductase gene. *PLoS One* 2012;**7**:13.

Urbina H, Schuster J, Blackwell M. The gut of Guatemalan passalid beetles: a habitat colonized by cellobiose- and xylose-fermenting yeasts. *Fungal Ecol* 2013;**6**:339–55.

Veiga A, Arrabaca JD, Loureiro-Dias MC. Cyanide-resistant respiration is frequent, but confined to yeasts incapable of aerobic fermentation. *FEMS Microbiol Lett* 2000;**190**:93–7.

Veiga A, Arrabaca JD, Sansonetty F *et al.* Energy conversion coupled to cyanide-resistant respiration in the yeasts *Pichia membranifaciens* and *Debaryomyces hansenii*. *FEMS Yeast Res* 2003;**3**:141–8.

Wohlbach DJ, Kuo A, Sato TK *et al.* Comparative genomics of xylose-fermenting fungi for enhanced biofuel production. *Pe Natl Acad Sci USA* 2011;**108**:13212–7.

Wright J, Bellissimi E, de Hulster E *et al.* Batch and continuous culture-based selection strategies for acetic acid tolerance in xylose-fermenting *Saccharomyces cerevisiae*. *FEMS Yeast Res* 2011;**11**:299–306.